Asian J. Exp. Sci., Vol. 33, No. 1, 2019; 1-20

Online available on :
www.ajesjournal.com, ISSSN : 0971-5444

Fore-arc Supra-subduction Setting for the Ophiolitic rocks from the Dizajaland area of the Khoy Ophiolite in West Azerbaijan, NW Iran

Leila Ebadi*, Seyed Mohammad Hosein Razavi and Hosein Sheikhi Karizaki
1Department of Geology, Azad University, North Tehran Branch, Tehran, Iran
* corresponding author; Email: leilaebadi_petro84@yahoo.com
Received: November 01, 2018; Revised: December 02, 2018; Accepted: December 14, 2018

Abstract : The ophiolitic rocks from the Dizajaland area in NW Iran are a part of the non-metamorphic ophiolitic complex of SW Khoy. They are close to eastern Turkey ophiolites, ophiolites along Zagros orogen and ophiolites from the Lesser Caucasus in Armenia. The study shows that all ophiolitic units including serpentinized peridotite, gabbro, diabase, pillow lavas and deep marine sediments are present in the area, although dismembered and displaced. Microfossils in the ophiolitic pelagic limestone indicate an age of Santonian-Campanian. Whole rock chemistry of the crustal sequence rocks indicates calk-alkaline to tholeiitic nature and a mid-ocean ridge to island arc tectonic-setting. The chemistry of the mafic rocks shows a mantle source, close to E-MORB compositions. The dual nature (i.e. both island arc and MORB) for the crustal sequence rocks, based on whole rock chemistry, is taken to represent a supra-subduction setting for these ophiolites. Mineral chemistry of orthopyroxene, spinel and olivine in the peridotites confirms a supra-subduction setting with a fore-arc environment for generation of these rocks. Ophiolitic rocks from the Dizajaland area can be considered as a continuation of "Inner Ophiolite Belt" of Iran, connecting it to the Izmir-Ankara-Erzincan suture. Apparently they are obducted along the Sevan-Akera suture in Armenia as a northern continuation of the Izmir-Ankara-Erzincan suture. These ophiolitic rocks are result of an intra-oceanic subduction with late Jurassic age.

Keywords: Ophiolite; supra-subduction zone; fore-arc; Neotethys; NW Iran

Introduction

The Iranian plateau is located along the Alpine-Himalayan orogenic belt. Based on geological structures, this plateau is divided into several units. Ophiolites and ophiolitic mélange complexes bordering some of these units appear widely in the Iranian crust (Fig. 1). Ophiolitic rocks along the Alborz mountain are taken as remnants of the Palaeotethys oceanic crust in north Iran (Alavi, 1991; Moghadam and Stern, 2014), while ophiolites along the Zagros mountain range, those from north of central Iran block and eastern Iran ophiolites are Neotethys-related ophiolites (Shafaii Moghadam and Stern, 2014; Arvin and Robinson, 1994; Dilek et al., 2007; Ghazi et al., 2010, 2011, 2012). Ophiolitic complexes, on NW Iran are exposed in the Chaldoran and Khoy area (Fig. 1). This area is one of the most complicated geological terrains in Iran and is a key area to reconstruct the geodynamics of Neotethys evolution. The geodynamic evolution and the connection of the Khoy ophiolite with the ophiolitic massifs of the Lesser Caucasus, NW Iran and East Anatolia still remain enigmatic (Avagyan et al., 2016). Khoy ophiolites, one of the largest ophiolitic complexes in Iran, is spatially close to Armenian ophiolites in the North, Zagros ophiolites in the south and eastern Turkey ophiolites in the west. Ophiolite from the Khoy area can be considered as continuation of Armenian ophiolites (continuation of Sevan-Akera suture, Avagyan et al., 2016 or south Azerbaijan suture, Topuz et al., 2013) continuation of Piranshahr ophiolites, which are displaced (therefore a part of Zagros-Bitlis suture) or as a part of Izmir-Ankara-Erzinca nature (north branch of southern Neotethys, e.g. Göncüoglu, 2014; Colako *et al.,* 2014) extended easterly to NW Iran. The clear relation of this ophiolite to the adjacent areas needs more investigations on its lithological nature, age and tectonic setting. Apparently Khoy ophiolite is outside of the so called "peri-Arabic ophiolite Belt" defined by Kniper et al. (1986). Hassanipak and Ghazi (2000) consider ophiolites in NW Iran equivalent to the inner group of Iranian ophiolites (e.g. Nain, Shahr-Babak, Sabzevar, Tchehel Kureh and Band-e-Zyarat, Fig. 1). They believe that they are formed as a result of closure of the northwestern branch of a narrow Mesozoic seaway.

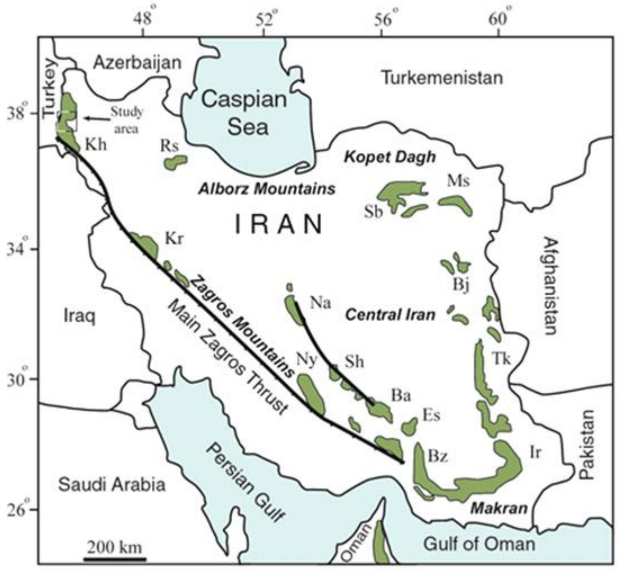

Fig. 1- Sketch map of Iran showing locations of the major ophiolites. Kh, Khoy; Km, Kermanshah; Ny, Neyriz; Bz, Band-e Zeyarat; Na, Nain; Bf, Baft; Sh, Shahr–Babak; Ir, Iranshahr; Tk, Tchehel Kureh; Ms, Mashad; Sb, Sabzevar; Rs, Rasht (Talesh ophiolite). (Modified after Ghazi *et al.,* 2012).

Ghazi and Hassanipak (2000) report a basal metamorphic zone beneath the Khoy ophiolite, displaying an inverse thermal gradient, ranging from the amphibolite facies to the greenschist facies (sole metamorphism). They present two ^{40}Ar–^{39}Ar plateau ages of 158.61.4 Ma and 154.91.0 Ma for hornblende gabbros, indicating formation of plutonic rocks of the Khoy ophiolite during Late Jurassic. They present also four ^{40}Ar–^{39}Ar plateau ages of ~104–110 Ma for hornblendes from the amphibolites of the basal metamorphic zone, giving a tectonic emplacement of Mid-Albian age for the ophiolite complex.

Khalatbari Jafari *et al.* (2003, 2004), studied the Khoy ophiolite in more details. They report two distinct ophiolitic complexes in the Khoy area (i) An older metamorphosed ophiolitic complex, at the eastern part of the area with Late Jurassic, Early Cretaceous age and (ii) A younger non-metamorphic ophiolite of Late Cretaceous age at the western part of the Khoy area (Fig. 2). The ophiolite outcrops in the Dizajaland area, to the south of the Khoy area (Figs. 2 and 3) are a part of the non-metamorphosed Khoy ophiolite.

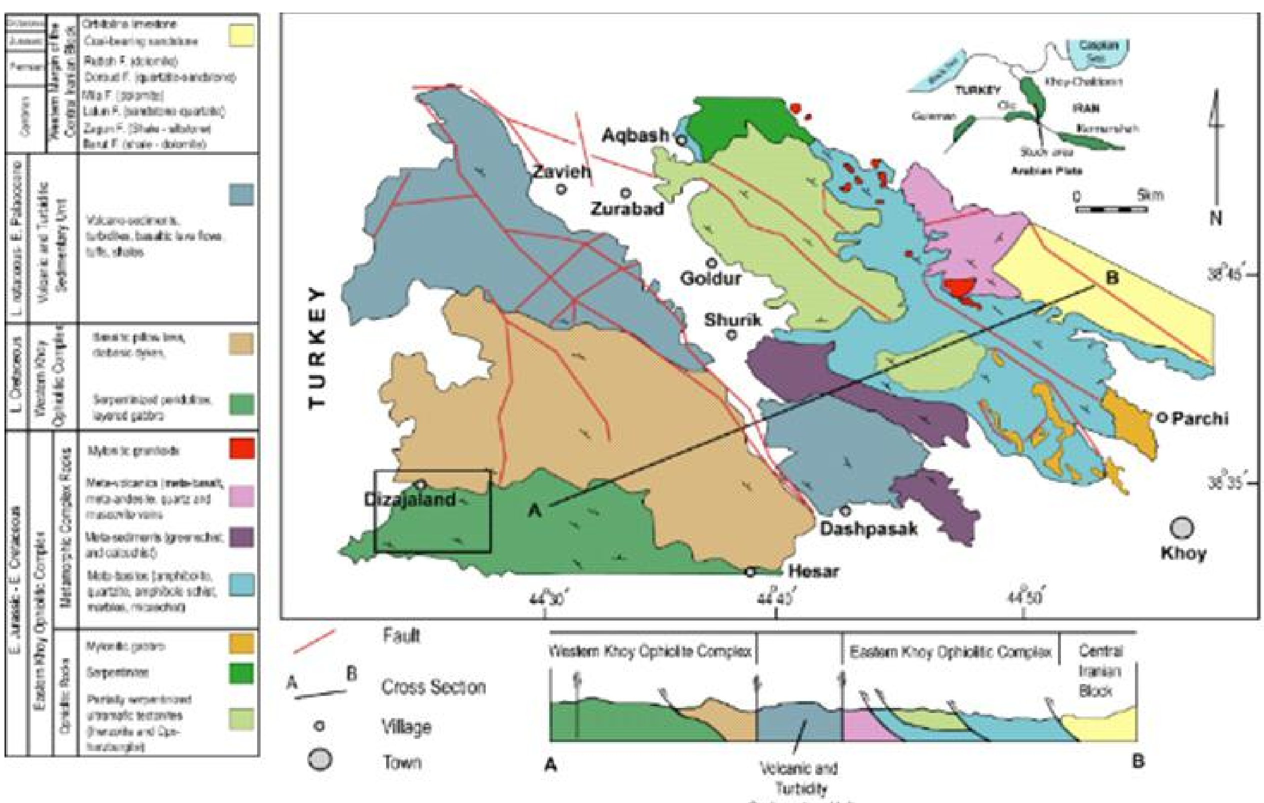

Fig. 2- General map of the Khoy area in NW Iran showing Western non-metamorphic ophiolite and Eastern metamorphic ophiolite complexes. The Dizajaland area is indicated by a rectangle (modified from Monsef *et al.,* 2010).

Although there are some publications on Khoy ophiolites and the related rocks (Khalatbari Jafari *et al*., 2003, 2004; Moazzen and Oberhänsli, 2008; Monsef *et al*., 2010; Azizi *et al*., 2011), but studies on the non-metamorphosed part is scarce. There is no published account on the petrography, geochemistry and tectonic setting of ophiolitic rocks from the Dizajaland area. In this contribution we provide new filed geology, petrography, whole rock and mineral chemistry data for this ophiolite in order to furnish more information for the relation of NW Iran ophiolites to the adjacent areas in a regional scale.

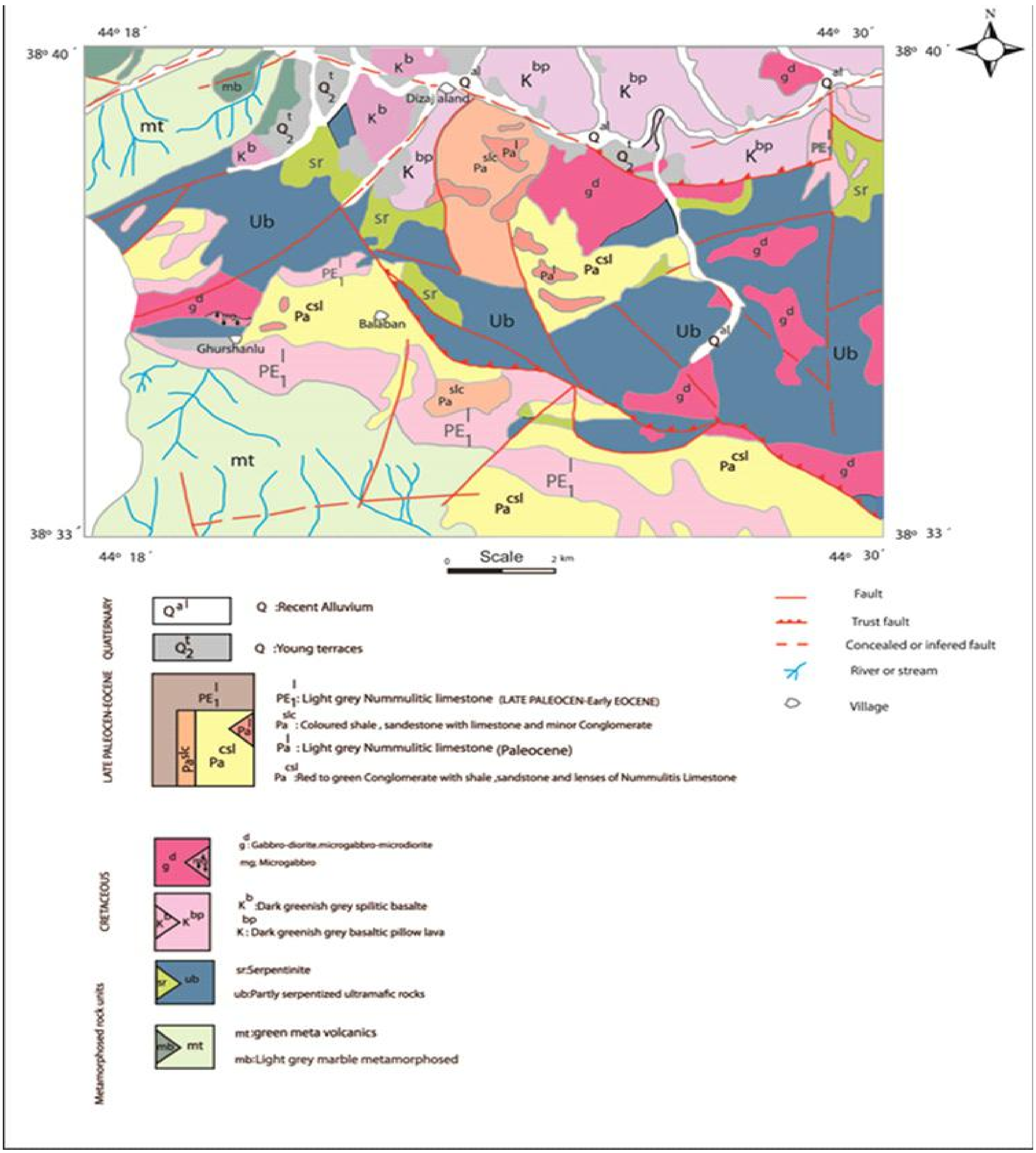

Fig. 3- Simplified geological map of the Dizajaland area (modified after Radfar *et al.,* 1993).

Geological Background

The oldest rock units in the Dizajaland area are metamorphic rocks including dark green amphibolites are composed mainly of hornblende and plagioclase, marble, calcschist, metavolcanics and greenschist (Fig. 3). The contact between the metamorphic rocks and other units are tectonic, therefore the stratigraphical relations are not clear. The age of these rocks is not known, but considering the fact that Mesozoic (Cretaceous) sedimentary rocks are not metamorphosed, the age of metamorphic rocks can be considered older than Cretaceous. The sedimentary rocks are Cretaceous unit with a thickness of 200-300m, composed of alternative layers of shale and siltstone (Fig. 4a). Rare limestone interclations occur occasionally between shales (Fig. 4a). Aplitic and diabasic dykes cut through the Mesozoic sedimentary rocks. Considering conglomerate intercalation, it can be concluded that the sedimentary basin was not deep. The lithological facies changes from deep sea pillow lavas to shallow one. Also the rocks are not metamorphosed. The shallow sedimentary rocks sit on reddish brown radiolarian chert at the northern part of the area. This points to a discontinuity at the base of the shallow Cretaceous sediments. Limestone and conglomerate of Paleocene to Eocene cover the Cretaceous sedimentary rocks with angular discontinuity in some places. Limestone interclations in the Cretaceous unit contains fossils (e.g. *Calcisphaerulaina minata, Stomisphaera spherical Pithonella trejoi, Stomiosphaelaconoides heterohelix spc.*) indicative of late Albian-Cenomanian age (Amini *et al*., 1993). The conglomerate part of this unit at the base, which sits discontinuously on radiolarian chert includes limestone lenses with *Globotruncana* and *Hedbergella* and Radiolarian fossils giving a possible age of Santonian to Campanian.

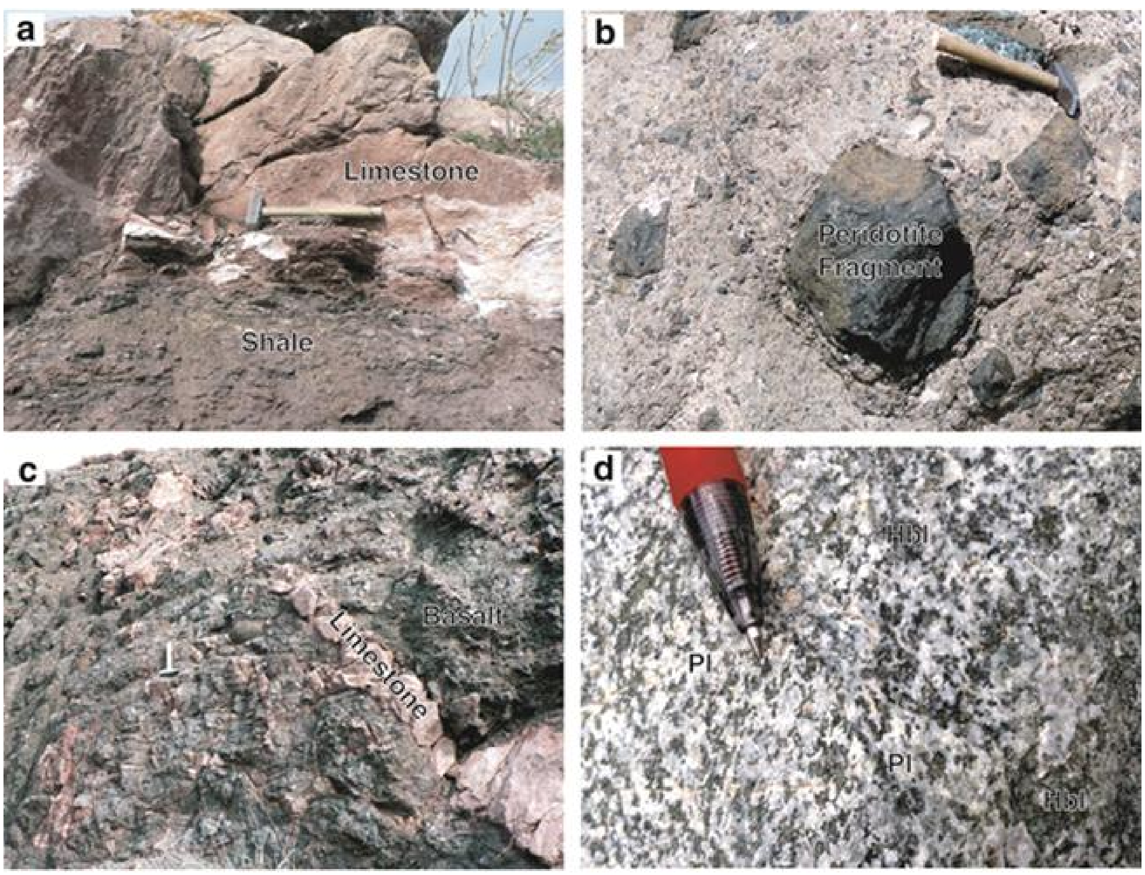

Fig. 4 (a-d) - Field photos of the ophiolitic and related rocks. **a)** Outcrop of Cretaceous limestone and shale. **b)** Paleocene conglomerate with serpentinized peridotite fragments. **c)** Pelagic limestone and spilitic basalt. **d)** Gabbro with visible plagioclase and plagioclase.

The Cenozoic rocks include Paleocene to Eocene units composed of ~350 m thick succession of shale, sandstone and limestone. The conglomerate fragments include basalt, gabbro, diorite and serpentinized peridotite (Fig. 4b), with weak sorting and roundness. These rocks cover older igneous rocks of the ophiolite complex (mainly gabbro-diorite and serpentinized peridotite). Limestone in this unit contains fossils of *Globotruncana, Aciculari* and miliolids, indicating a late Paleocene age.

The ophiolitic rocks of the Dizajaland area are composed of serpentinized peridotites, serpentine, gabbro, diabase, spilitic pillow lava, radiolarian chert and Santonian-Campanian pelagic limestone (Figs. 4 and 5). The serpentinized peridotites and serpentinites occur at the middle part of the study area. Large blocks of gabbro can be seen in association with serpentinized peridotites. Pillow basalt occupy a large area at north of the study area.

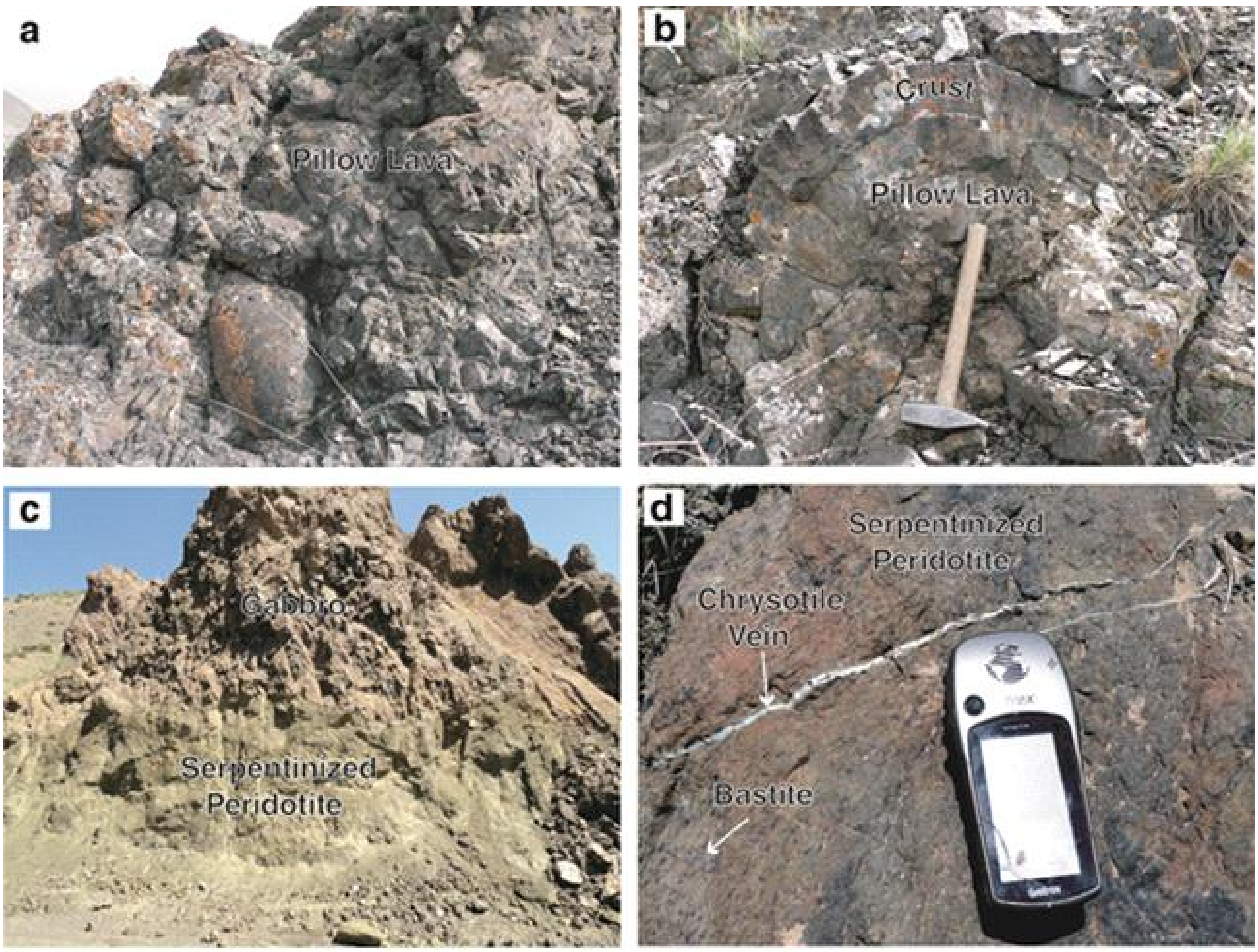

Fig. 5-a-d : **a)** Outcrop of pillow basalts. **b)** A close view of a pillow with child crust. **c)** Gabbro overlying serpentinized peridotite**. d)** A close view of serpentinized peridotite with bastite after original pyroxene

Petrography of Ophiolitic Rocks

Basalt and Diabase

The basaltic rocks of the area are lavas with pillow structure. Diabasic rocks appear as dykes cutting mainly gabbros. Basalts are dark colour in hand specimen and have porphyry and microlitic porphyry textures under the microscope (Fig. 6-a). The main minerals are plagioclase and clinopyroxene. Plagioclase is slightly altered to sericite and clinopyroxene shows alteration to chlorite and oxide minerals (Fig. 6-a). The minor phases include opaque minerals, titanite and occasionally chert, chlorite and calcite, filling the vesicles. Diabase samples are dark green to grey in hand specimen and have doleritic texture under the microscope (Fig. 6-b). They are composed of plagioclase, clinopyroxene and amphibole. Plagioclase is slightly altered to sericite and clay minerals, while clinopyroxene is altered to chlorite and opaque minerals. The minor phases are titanite and oxide minerals.

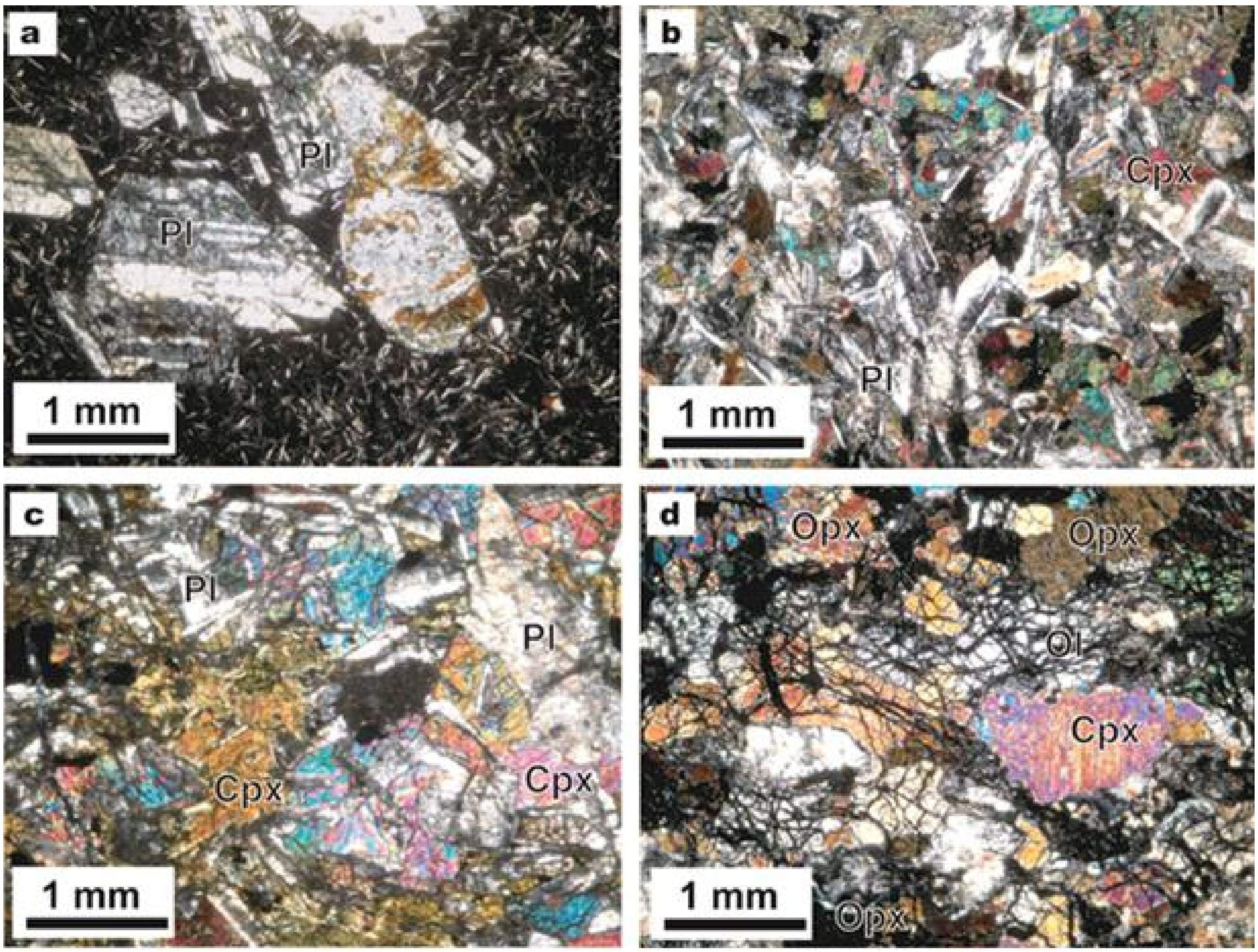

Fig. 6 a-d): Microscopic images of the representative samples. a) Basalt with plagioclase phenocrysts and fine-grained groundmass (XPL). b) A diabase with clinopyroxene and plagioclase (XPL). c) Gabbro with relatively large crystals of clinopyroxene and plagioclase (XPL). d) Partially serpentinized peridotite with olivine and pyroxene crystals.

Gabbro

The gabbroic rocks of the Dizajaland area are either gabbro or gabbro-diorite (Fig. 6-c). They appear as both massive rocks and layered gabbros. The main texture in the rocks are intergranular and poikilitic textures. The mineral constituents of the gabbros are plagioclase, slightly altered tosericite, chlorite and epidote and clinopyroxene with idiomorphic to sub-idiomorphic crystals, which are uralitized. The clinopyroxenes are changed to tremolite-actinolite at the rims. Minor phases are opaque minerals, titanite and apatite.

Serpentinized Peridotites

The peridotites are composed of olivine, orthopyroxene, clinopyroxene and spinel (Fig. 6-d). Considering the modal proportion of these minerals, three types of peridotites can be recognized. These are harzburgite, dunite and pyroxenite. These serpentinized peridotites can be divided into two main groups, based on the degree of serpentinization, which are peridotites with low serpentinization and those which are highly serpentinized. Olivine in harzburgite is changed to serpentine and opaque minerals and remaining of olivine is preserved in the core of mesh textures. Clinopyroxene and orthopyroxene are also altered to serpentine minerals. Spinel appears mainly as red crystals (picotite) along with subordinate amounts of titanite. Based on optical properties, serpentine polymorphs developed in the rocks are lizardite and chrysotile.

Whole Rock Geochemistry

Seven representative samples of mafic rocks from the crustal sequence of ophiolite in the Dizajaland area were analyzed for major oxides and trace elements. Three basalt, three gabbro and one diabase samples were analyzed. About 1kg of each sample was crushed and pulverized to smaller than 200 m, then was fused by lithium metaborate. The resulted bids were used for XRF analyses and they dissolved in acid and were analyzed by ICP-MS method. The analyses were carried out in the Actlabs Company, Canada. Uncertainties are better than ±2% for the major oxides and ±5% for the trace elements. The results are shown in Table 1.

Table 1- Major oxides and trace elements of the analysed basalt (LE4, LE8A, LE8B, LE8C,LE15A,LE15B, LE15C, LE15D) and gabbro (LE9B, LE11K, LE12F) samples. Major oxides in wt% and trace elements in ppm.

Sample	LE4	LE9B	LE11K	LE12F	LE8A	LE8B	LE8C	LE15A	LE15B	LE15C	LE15D
SiO_2	48.33	48.62	47.32	43.6	48.69	48.29	49.82	48.21	48.42	47.98	48.33
Al_2O_3	19.3	15.17	15.21	21.73	15.56	16.78	16.54	15.11	16.81	16.08	15.91
$Fe2O_3(T)$	8.53	11.6	10.73	4.94	10.62	9.25	9.37	12.04	9.12	9.22	9.16
MnO	0.128	0.186	0.177	0.092	0.143	0.138	0.141	0.178	0.128	0.133	0.137
MgO	5.67	6.73	7.44	9.3	5.94	5.64	3.83	6.22	5.59	5.91	6.12
CaO	11.9	9.05	10.93	15.39	10.91	11.43	13.39	9.16	11.32	11.28	10.24
Na_2O	2.95	3.47	3.25	0.53	3.25	3.4	2.8	3.63	3.7	3.6	3.55
K2O	0.19	0.58	0.65	0.32	0.19	0.26	0.09	0.49	0.27	0.23	0.26
TiO_2	1.043	1.581	1.31	0.059	1.548	1.4	1.419	1.66	1.4	1.35	1.42
P_2O_5	0.08	0.19	0.13	< 0.01	0.16	0.14	0.18	0.21	0.15	0.15	0.17
LOI	2.76	3.75	3.52	3.12	2.8	4	3.38	3.71	3.31	3.33	3.61
Total	100.9	100.9	100.7	99.08	99.81	100.7	101	100.618	100.218	99.263	98.907
Sc	32	37	41	24	38	35	36	33	32	36	37
Be	< 1	< 1	< 1	< 1	< 1	< 1	< 1	< 1	< 1	< 1	< 1
V	206	272	299	64	270	248	255	288	261	277	245
Ba	22	102	40	123	40	36	34	111	35	110	98
Sr	213	339	165	169	243	313	232	421	322	303	351
Y	21	28	27	2	25	22	22	27	21	20	25
Zr	58	108	76	4	91	84	89	102	75	84	96
Cr	280	250	250	210	220	230	220	261	260	276	270
Co	38	44	42	36	40	40	57	41	38	35	39
Ni	90	70	110	60	60	70	80	68	66	67	68
Cu	110	90	100	30	100	100	90	90	81	83	87
Zn	60	80	80	< 30	80	70	80	83	62	60	63
Ga	18	19	18	12	20	18	18	19	17	15	17
Ge	2	2	2	1	2	2	2	3	2	2	2
As	< 5	< 5	< 5	< 5	< 5	< 5	< 5	< 5	< 5	< 5	< 5
Rb	3	6	17	2	< 2	4	< 2	5	5	2	5

Nb	<1	5	2	< 1	6	5	5	5	5	2	5
Mo	< 2	< 2	< 2	< 2	< 2	< 2	< 2	< 2	< 2	< 2	< 2
Ag	< 0.5	< 0.5	< 0.5	< 0.5	< 0.5	< 0.5	< 0.5	< 0.5	< 0.5	< 0.5	< 0.5
In	< 0.2	< 0.2	< 0.2	< 0.2	< 0.2	< 0.2	< 0.2	< 0.2	< 0.2	< 0.2	< 0.2
Sn	4	4	4	3	4	3	3	3	3	4	3
Sb	< 0.5	< 0.5	< 0.5	< 0.5	< 0.5	< 0.5	< 0.5	< 0.5	< 0.5	< 0.5	< 0.5
Cs	< 0.5	< 0.5	9.8	< 0.5	< 0.5	< 0.5	< 0.5	< 0.5	< 0.5	< 0.5	< 0.5
La	2.8	7.5	5.5	0.3	6.8	6.6	6.2	7.7	6.9	6.6	6.8
Ce	8	18.6	13.4	0.6	17.3	16.3	15.5	19.1	16.5	17.2	16.63
Pr	1.35	2.8	2.01	0.08	2.59	2.43	2.31	2.4	2.31	2.21	2.14
Nd	7	13.6	9.8	0.3	12.3	11.3	11.2	12.9	11.1	13.1	12.8
Sm	2.5	4.1	3.1	0.2	3.7	3.3	3.4	4.3	3.1	2.9	2.5
Eu	1.01	1.5	1.25	0.08	1.43	1.27	1.3	1.6	1.22	1.23	1.31
Gd	3.2	4.8	4.1	0.2	4.3	4	3.9	5.1	4.7	4.1	4.4
Tb	0.6	0.9	0.8	< 0.1	0.8	0.7	0.7	0.8	0.6	0.7	0.7
Dy	3.8	5.2	4.8	0.2	5	4.3	4.1	5.1	4.4	4.8	5
Ho	0.8	1.1	1	< 0.1	1	0.9	0.8	1.1	0.9	1.1	1.2
Er	2.3	3.1	3	0.2	2.9	2.5	2.4	3.3	2.2	2.4	2.9
Tm	0.35	0.49	0.48	< 0.05	0.43	0.38	0.37	0.43	0.39	0.41	0.38
Yb	2.3	3	3.1	0.2	2.8	2.4	2.3	2.9	2.1	2.8	2.4
Lu	0.33	0.41	0.44	< 0.04	0.39	0.33	0.32	0.44	0.3	0.3	0.4
Hf	1.7	2.7	2	< 0.2	2.6	2.4	2.2	2.4	2.7	2.2	2.5
Ta	< 0.1	0.3	0.4	< 0.1	0.3	0.3	0.3	0.3	0.3	0.3	0.3
W	< 1	< 1	< 1	< 1	< 1	< 1	3	< 1	< 1	< 1	< 1
Tl	< 0.1	< 0.1	< 0.1	< 0.1	< 0.1	< 0.1	< 0.1	< 0.1	< 1	< 1	< 1
Pb	< 5	< 5	< 5	< 5	< 5	< 5	< 5	< 5	< 5	< 5	< 5
Bi	< 0.4	< 0.4	< 0.4	< 0.4	< 0.4	< 0.4	< 0.4	< 0.4	< 0.4	< 0.4	< 0.4
Th	0.2	0.7	0.5	< 0.1	0.6	0.6	0.6	0.8	0.8	0.6	0.8
U	< 0.1	0.2	0.2	< 0.1	0.2	0.2	0.2	< 0.1	0.2	< 0.1	< 0.1

Gabbro samples show calc-alkaline nature, while basalt and diabase samples are tholeiitic (Fig. 7-a). In order to find out the tectonic setting of the studied mafic rocks, immobile trace elements were used. Based on Ti, Zr and Sr content of the studied rocks (Pearce and Cann, 1973), diabasic sample plot in the island arc setting and gabbro and basalt samples plot in both mid ocean ridge and island arc fields (Fig. 7-b). On the Th/Nb versus Nb/Y diagram (Kamenov, 2004), samples from pillow basalts and gabbros plot close to E-MORB (except for one sample) and the diabasic sample plots close to N-MORB (Fig. 7-c). Pearce (2008) proposed diagrams to distinguish basalts from ophiolites with mid-ocean ridge setting and those from supra-subduction setting. Diagram of Th/Yb versus Ta/Yb is used in this regard (Fig. 7-d).

Most of the samples plot in the supra-subduction zone in this diagram, and at the border of calc-alkaline and tholeiitic fields. As can be seen, the mafic rocks of the ophiolites in the Dizajaland area show dual geochemical features indicative of mafic rocks formed at mid-ocean ridge and to those formed in a subduction zone. These mixed features can be found in mafic rocks from supra-subduction zone ophiolites (e.g. Cyprus, Floyd *et al.,* 1998; Oman, Rollinson, 2009; Piranshahr, Hajialioghli and Moazzen, 2014).

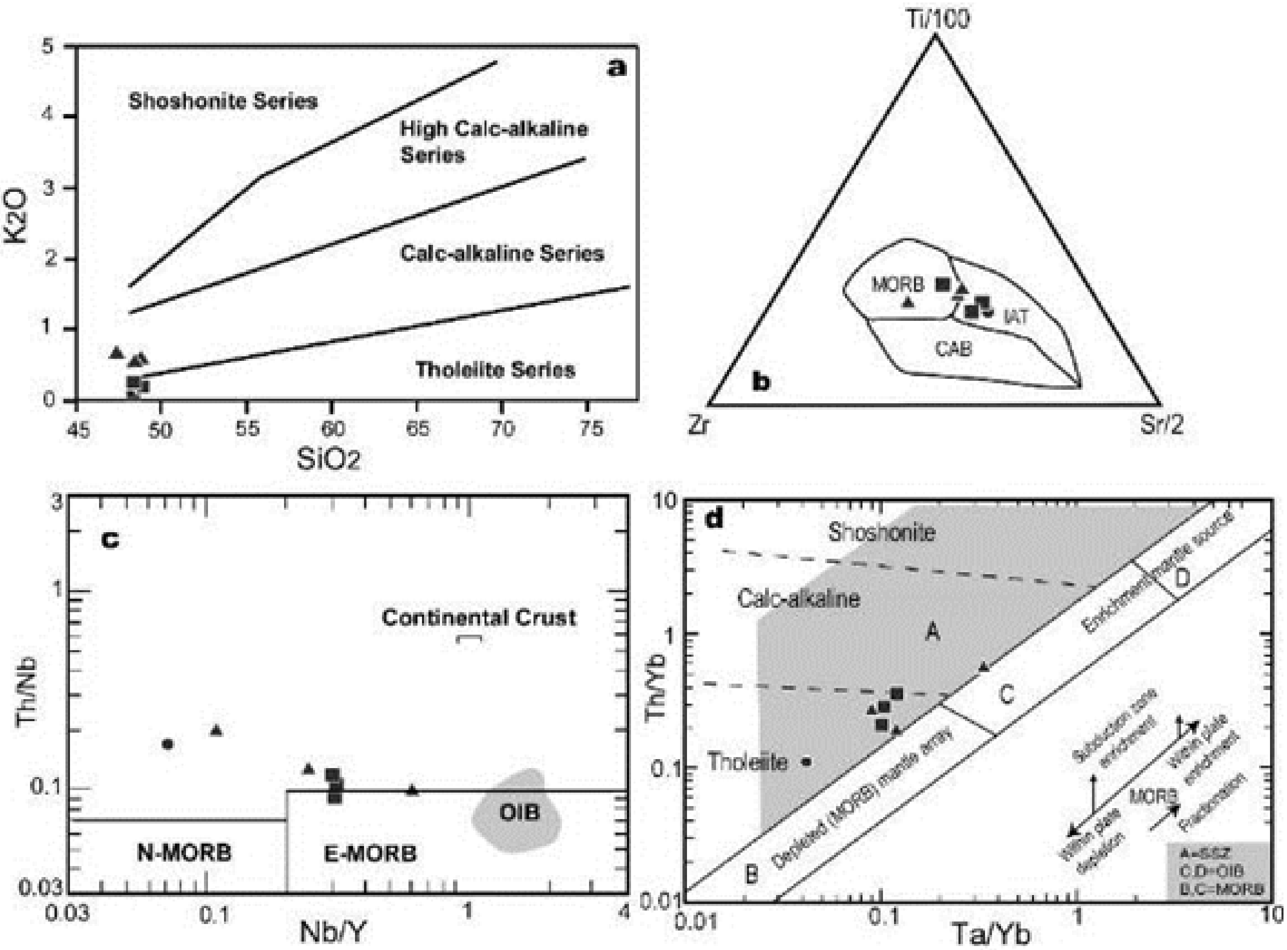

Fig. 7 a-d) - **a)** The studied mafic rock from the crustal sequence show tholeiitic to clac-alkaline nature. **b)** The analysed samples plot in the MORB and IAT diagram of Pearce and Cann (1973). **c)** Diagram of Kamenov (2004) on which the studied samples close to N-MORB and E-MORB fields. **d)** Diagram of Pearce (1982) indicates a supra-subduction zone setting for the Dizaj-Al and mafic rocks with tholeiitic to calc-alkaline nature. For more details see the text.

REE contents of the studied rocks are normalized to chondrite (Sun and McDonough, 1989). The diabasic sample shows a gentle enrichment from La to Sm and a flat pattern from Sm to Lu on the REE diagram (Fig. 8). All basalt and gabbro samples resemble E-MORB REE pattern (except for one gabbro sample). On the spider diagram normalized to primary mantle values (Sun and McDonough, 1989), gabbro and diabase samples show negative Nb anomalies with enrichment in U, Pb K ad Sr with a relatively flat pattern from Sm to Lu (Fig. 9).

Basalt samples do not exhibit the negative Nb anomaly. One of the geochemical features of the mafic rocks from the subduction zones is negative anomaly of TNT (Ti, Nb, Ta) (Wilson, 1989), which shows that these elements are preserved in the source materials during partial melting. Refractory phases such as ilmenite and rutile remaining in the subducting slab, accumulate HFSE such as Ti, Nb and Zr, preventing entrance of these elements into the resulted melt, which in turn results in depletion of these elements in the generated rocks Bogoch *et al*., 2002). However, these negative anomalies can also be produced by contribution of continental materials (Sun 1980; Saunders *et al*., 1992). High ratios of Ba/Zr are indicative of continental contamination. This ratio is 2-5 for continental basalts (Fitton *et al.*, 1998), while it is ~ 0.8 for MORB and 1.25 for ocean island basalt (Sun and McDonough, 1989). This ratio is 0.3-0.8 for the studied basalts, close the MORB values. Therefore, Nb depletion more likely is not due to continental materials contamination and instead

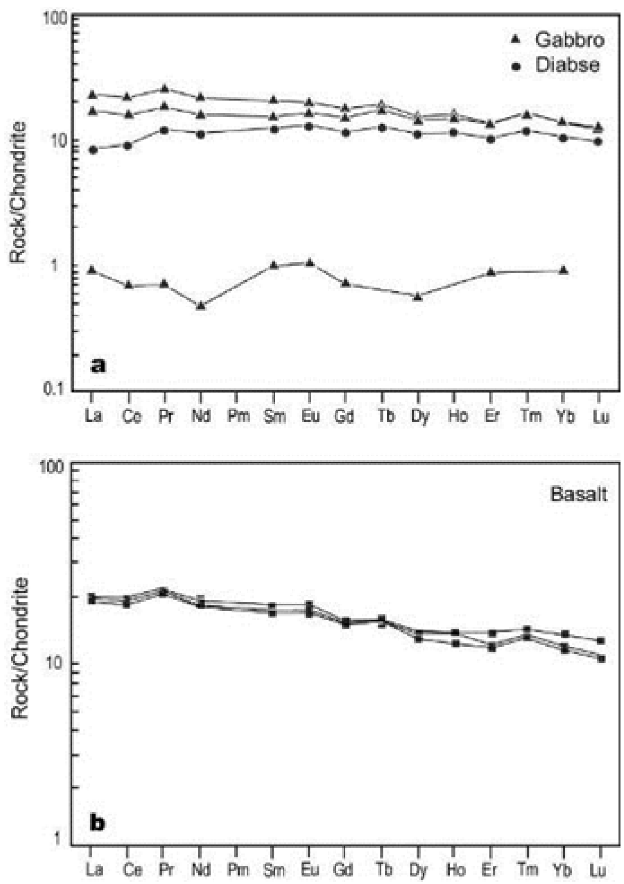

Fig. 8 - REE diagrams for the mafic rocks, showing relatively flat pattern with slight enrichment of LREE. The normalizing factors are from Sun and McDonough (1989).

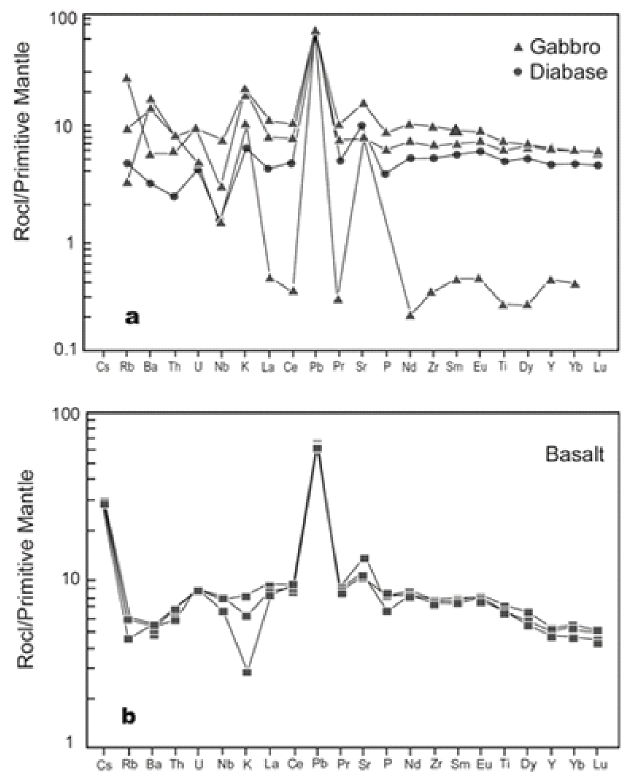

Fig.9 - Spider diagrams for the mafic rocks with pronounced Pb positive anomaly, more likely due to influence of crustal-derived materials in the supra-subduction zone setting. the normalizing factors are from Sun and McDonough (1989).

testifies for a subduction zone source (mantle wedge) for the Dizajaland basalts. This is in agreement with a supra-subduction setting for the studied ophiolite.

Mineral Chemistry

Minerals in five representative samples of peridotites and gabbros were analysed using a JEOL JXA-8100 electron probe micro analyzer in the Analytical Laboratory of the Beijing Research Institute of Uranium Geology, Beijing, China. The accelerating voltage was 20 kV and specimen current was 10 nA with 2 m beam diameter. Counting time on peaks and half peaks was 10s. Natural and synthetic standards were used for calibration. Analytical results are provided in Tables 2 to 4.

Table 2- Representative analyses of olivine in Dizajaland peridotites. The formula is calculated based on of 4 oxygen atoms.

Sample Elements	LE11E	LE11E	LE12A	LE12A	LE12G	LE12G	LE12G	LE12N	LE12N	LE12N	LE12N
SiO_2	41.20	41.80	39.20	39.60	39.70	39.80	39.60	39.60	38.40	39.30	38.50
TiO_2	BD	BD	BD	BD	BD	BD	0.06	BD	BD	BD	0.06
Al_2O_3	BD	BD	BD	0.01	0.01	BD	BD	BD	BD	0.03	BD
Cr_2O_3	BD	BD	BD	BD	BD	0.04	BD	0.04	BD	BD	BD
FeO	8.30	8.40	16.60	16.90	16.40	16.30	15.70	15.30	15.80	16.30	16.60
MnO	0.12	0.17	0.29	0.27	0.32	0.23	0.28	0.19	0.30	0.20	0.29
MgO	51.70	51.10	43.90	43.60	44.30	43.60	44.60	44.90	43.90	43.60	43.20
CaO	0.05	0.03	BD	0.01	BD	BD	BD	0.03	0.03	0.03	0.02
Na_2O	0.02	BD	BD	BD	BD	0.04	BD	BD	BD	BD	BD
K_2O	0.01	0.01	BD	0.03	BD	99.10	BD	BD	BD	BD	BD
Total	101.40	101.51	99.99	99.39	100.73	100.01	100.24	100.06	98.43	99.46	98.67
Si	1.001	1.001	0.992	0.998	0.995	1.005	0.996	0.995	0.986	0.999	0.989
Ti	0.000	0.000	0.000	0.000	0.000	0.000	0.001	0.000	0.000	0.000	0.001
Al	0.000	0.000	0.000	0.000	0.000	0.000	0.000	0.000	0.000	0.001	0.000
Cr	0.000	0.000	0.000	0.000	0.000	0.001	0.000	0.001	0.000	0.000	0.000
Fe^{2+}	0.165	0.168	0.352	0.357	0.345	0.343	0.330	0.321	0.339	0.346	0.357
Mn	0.002	0.003	0.006	0.006	0.007	0.005	0.006	0.004	0.007	0.004	0.006
Mg	1.829	1.825	1.657	1.640	1.657	1.640	1.670	1.683	1.681	1.650	1.656
Ca	0.001	0.001	0.000	0.000	0.000	0.000	0.000	0.001	0.001	0.001	0.001
Na	0.001	0.000	0.000	0.000	0.000	0.002	0.000	0.000	0.000	0.000	0.000
K	0.000	0.000	0.000	0.001	0.000	0.000	0.000	0.000	0.000	0.000	0.000
Total	2.999	2.998	3.007	3.002	3.004	2.996	3.003	3.005	3.014	3.001	3.010

Table 3- Representative analyses of orthopyroxene in Dizajaland peridotites. The formula is calculated based of 6 oxygen atoms.

Sample Elements	LE11E	LE11E	LE11E	LE11E	LE11E	LE11E	LE11E	LE11E
SiO_2	56.72	57.15	57.05	56.92	57.55	56.77	57.89	57.50
TiO_2	BD	0.06	0.08	0.11	BD	0.09	BD	BD
Al_2O_3	1.46	1.35	1.48	1.36	1.33	1.36	1.18	1.46
Cr_2O_3	0.68	0.61	0.72	0.52	0.57	0.54	0.54	0.64
FeO	5.37	5.18	4.89	5.07	5.15	5.33	5.08	4.80
MnO	0.19	0.14	0.12	0.15	0.16	0.13	0.10	0.13
MgO	34.24	34.62	33.00	34.18	34.69	34.53	36.16	35.02
CaO	1.37	1.43	2.86	0.85	1.41	1.02	1.02	1.15
Na_2O	BD	BD	BD	BD	BD	BD	BD	BD
K_2O	0.01	BD	BD	BD	BD	BD	0.01	0.01
Total	100.04	99.11	100.20	99.16	100.86	99.77	101.98	100.71
Si	1.953	1.956	1.968	1.975	1.964	1.957	1.956	1.961
Ti	BD	0.002	0.002	0.003	BD	0.002	BD	BD
Al	0.059	0.053	0.060	0.056	0.053	0.055	0.046	0.059
Cr	0.019	0.017	0.020	0.014	0.015	0.015	0.014	0.017
Fe^{3+}	0.016	0.014	BD	BD	0.004	0.013	0.028	0.003
Fe^{2+}	0.138	0.135	0.160	0.170	0.143	0.141	0.113	0.134

Mn	0.006	0.004	0.004	0.004	0.005	0.004	0.003	0.004
Mg	1.758	1.767	1.697	1.768	1.764	1.774	1.803	1.780
Ca	0.051	0.052	0.106	0.032	0.052	0.038	0.036	0.042
Na	BD	BD	0.002	0.002	BD	0.001	BD	BD
K	BD	BD	BD	BD	BD	BD	BD	BD
Total	4.000	4.000	4.019	4.024	4.000	4.000	3.999	4.000
$Mg/(Mg+Fe^{2+})$	0.927	0.929	0.914	0.912	0.925	0.927	0.941	0.930
$Fe^{2+}/(Fe_{tot})$	0.896	0.908	1.133	1.154	0.973	0.916	0.799	0.978
$Al/(Al+Fe^{3+}+Cr)$	0.631	0.644	0.985	1.179	0.734	0.666	0.520	0.743
En	0.903	0.904	0.865	0.898	0.901	0.909	0.924	0.910
Fs	0.071	0.069	0.081	0.086	0.073	0.072	0.058	0.068
Wo	0.026	0.027	0.054	0.016	0.026	0.019	0.019	0.021
Jd	0.000	0.000	0.002	0.002	0.000	0.001	0.000	0.000
Ac	0.000	0.000	0.000	0.000	0.000	0.000	0.000	0.000
Aug	1.000	1.000	0.998	0.998	1.000	0.999	1.000	1.000

Table 4- Representative analyses of spinel in Dizajaland peridotites
.formula is calculated based of 4 oxygen atoms

Sample Elements	**LE11E**	**LE11E**	**LE11E**	**LE11E**
TiO_2	0.18	BD	0.13	0.07
Al_2O_3	20.39	20.85	20.55	20.87
Cr_2O_3	48.17	47.73	48.80	47.55
FeO	17.47	17.72	17.48	18.18
MnO	0.31	0.29	0.21	0.26
NiO	0.10	0.00	0.04	0.04
MgO	13.61	13.25	13.46	12.83
Total	**100.23**	**99.84**	**100.67**	**99.80**
Ti	0.004	0.000	0.003	0.002
Al	0.739	0.759	0.743	0.762
Cr	1.172	1.166	1.184	1.165
Fe^{3+}	0.080	0.075	0.067	0.070
Fe^{2+}	0.369	0.382	0.381	0. 401
Mn	0.008	0.008	0.005	0.007
Ni	0.002	0.000	0.001	0.001
Mg	0.624	0.610	0.616	0.593
Total	2.998	3.000	3.000	3.001
$Mg/(Mg+Fe^{2+})$	0.628	0.615	0.618	0.596
$Fe^{2+}/(Fe^{2+}+Fe^{3+})$	0.821	0.835	0.850	0.852
$Al/(Al+Fe^{3+}+Cr)$	0.371	0.379	0.373	0.382

Olivine in the Dizajaland peridotites is Mg-rich (Table 2). MgO is between 43.20 and 51.70 wt% in different samples, while the composition of olivine is almost homogeneous in each sample. TiO_2 and Cr_2O_3 contents are very low (mainly blow the detection limit).

The analysed orthopyroxenes have $Mg^{\#}$ of ~0.9 and Cr_2O_3 content of 0.3-0.7 (Table 3). TiO_2 contents are 0.10 to 0.06. They appear as homogenous crystals without chemical zoning.

The spinels are Cr-spinel (Table 4) with FeO contents of 17.47-18.18 wt% and MgO contents of 12.83-13.61 wt%. $Mg^{\#}(Mg/(Mg+Fe^{2+})$ of spinels is ~0.6.

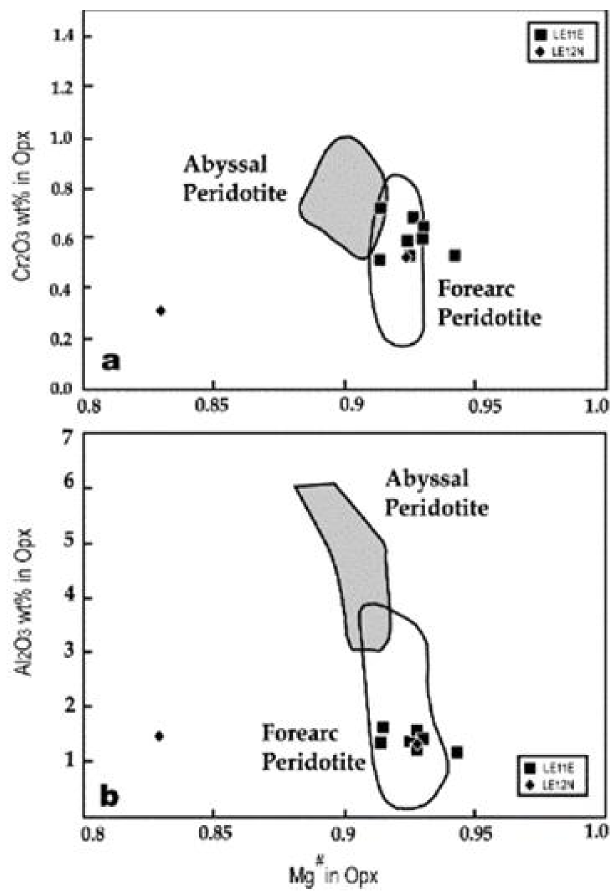

Fig. 10- Mineral chemistry of orthopyroxene in the peridotites indicating a fore-arc setting for the rocks. Fields for abyssal peridotites is from Johnson *et al.,* (1990) and fore-arc peridotites from Ishii *et al.* (1992).

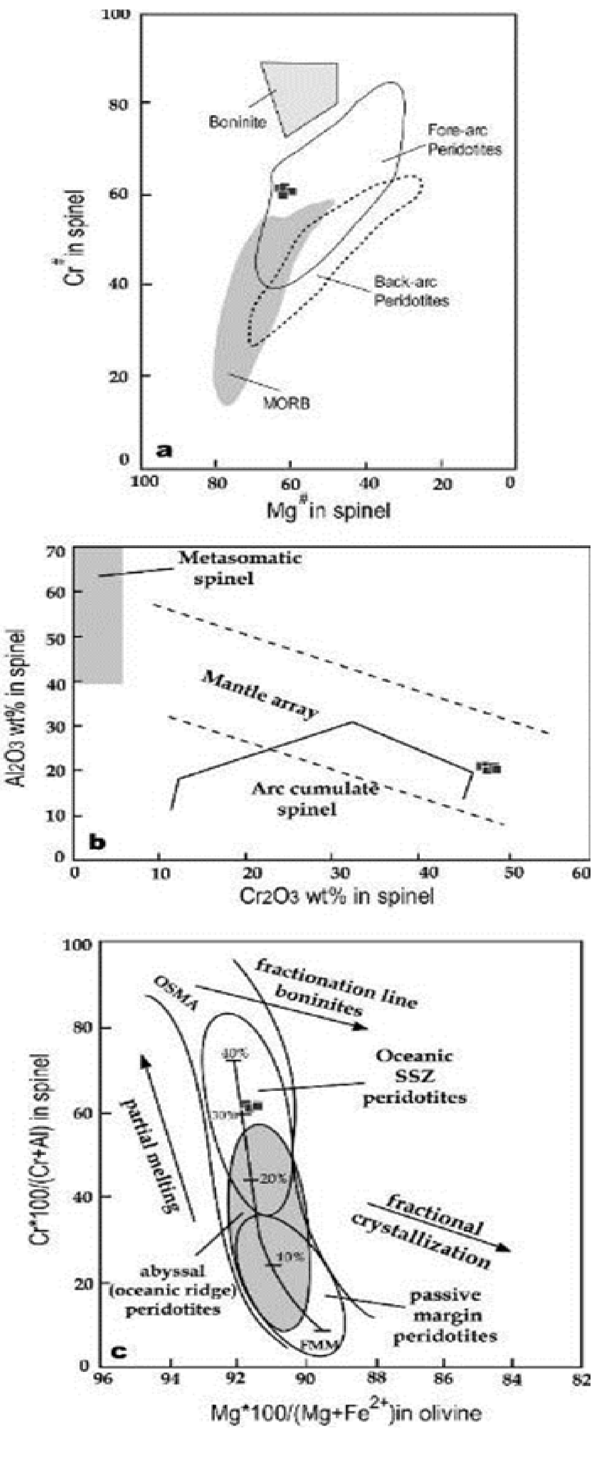

Fig. 11 a-c) - **a)** Spinel chemistry confirms a fore-arc setting for the peridotites. **b)** Al_2O_3 versus Cr_2O_3 diagram in which the analysed samples plot in the mantle array (Conrad and Kay, 1984; Haggerty, 1988; Kepezhinskas *et al.,* 1995). **c)** The studied rocks plot in the oceanic supra-subduction zone peridotites diagram of Arai (1987, 1994 a, b).

Using criteria proposed by Johnson *et al.* (1990), Ishii *et al.* (1992) and Choi *et al.* (2008), the analysed orthopyroxene chemistry shows a supra-subduction and fore-arc setting for the Dizajaland ophiolite (Fig. 10). Cr# versus Mg# in spinels from the Dizajal and peridotites confirms a fore-arc setting for these rocks (Fig. 11a). Cr_2O_3 versus Al_2O_3 of spinels define a mantle array (Fig. 11b) for the studied rocks (Conrad and Kay, 1984; Haggerty, 1988; Kepezhinskas *et al*., 1995). Based on $Cr^{\#}$ and $Mg^{\#}$ of spinel (Arai, 1987, 1994 a, b), the Dizajaland peridotites plot in the olivine-spinel of mantle array (OSMA) (Fig. 11c). This diagram shows that the spinels are mantle residua.

Discussion

Dizajaland ophiolitic rocks in NW Iran are a part of the non-metamorphic western Khoy ophiolite. The crustal sequence is composed of gabbro, diabasic dykes and pillow lava. The mantle sequence is mainly composed of low clinopyroxene-bearing harzburgite and subordinate amounts of pyroxenite and dunite, serpentinized to different degrees. Whole rock chemistry of the crustal sequence rocks of this ophiolite indicates a supra-subduction zone and island arc setting for the ophiolite. Mineral chemistry of olivine, orthopyroxene and spinel in the harzburgitic peridotites confirms a fore-arc supra-subduction setting for the ophiolites. Characteristic mineral chemistry of low Cpx-bearing harzburgites includes the high $Cr^{\#}$ of the spinels and high $Mg^{\#}$ but low$Al_2O_3$and Na_2O content of orthopyroxenes. Major and trace element whole rock chemistry of the mafic rocks also is more compatible with formation of ophiolites in a supra-subduction zone.

Hassanipak and Ghazi (2000) consider the Khoyo phiolite equivalent to the inner group of Iranian ophiolites (including Nain, Shahr-Babak, Sabzevar, Tchehel Kureh and Band-e-Zeyarat), formed at a spreading center in an arrow Mesozoic seaway that once surrounded the Central Iranian microcontinent. This is concluded based on similarities of chemistry of basalts from the Khoy ophiolite to those of some Iranian 'inner ophiolites' (Hassanipak and Ghazi, 2000). They rule out equating the Khoy ophiolite with ophiolites along Bitlis-Zagros suture due to of lack of a major tectonic element responsible for Khoy ophiolite displacement**.**

Khalatbari Jafari *et al.* (2003) reported Upper Cretaceous age for the western part of the Khoy ophiolite (Younger non-metamorphic Khoy ophiolites, Khalatbari Jafari *et al.,* 2003), based on the abundant microfauna in the pelagic limestones interbedded within volcanic rocks and also K/Ar dating on plagioclase in leucogabbroic veins in the layered gabbros. According to them, the stratigraphy and structural relations in the non-metamorphic ophiolite is typical of a slow-spreading ridge environment. They excluded a possible supra-subduction setting for the Khoy ophiolite. Monsef *et al.* (2010) considered a supra-subduction setting in relation to a slow-spreading back-arc basin for the Khoy ophiolite, based on geochemical and microstructural features on the serpentinized peridotites. Moazzen *et al.* (2012) also considered a supra-subduction setting for the Khoy ophiolites based on mineral chemistry of peridotites of the non-metamorphic complex. They considered the Khoy ophiolite as a continuation of the Iranian "Inner Ophiolites" connecting them to the ophiolites along the Izmir-Ankara-Erzincan suture in Turkey (Fig. 12).

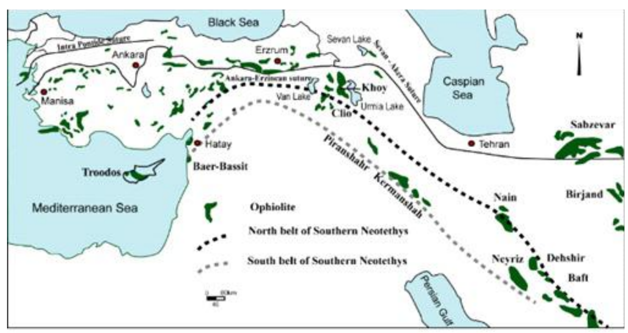

Fig. 12- Distribution of ophiolites, ophiolitic melanges and ophiolitic belts in Iran, Armenia and Turkey (modified from Çolako lu *et al.,* 2014).

Colako lu *et al.* (2014) and Göncüoglu (2014) discussed the possible relation of Turkish ophiolites towards the east to the Iranian ophiolites (Fig. 12). They consider the "North Ophiolite Belt, NOB" of Turkey as continuation of "Inner Ophiolite Belt" of Iran to the north of Pütürge- Bitlis and Sanandaj-Sirjan zone respectively and "South Ophiolite Belt, SOB" of Turkey as the continuation of the "Outer Ophiolite Belt" of Iran to the south of Pütürge- Bitlis and Sanandaj-Sirjan zone respectively. The situation of the Khoy ophiolite is not clear in their studies. They consider the Khoy ophiolite as an exception along the NOB of Turkey and its continuation in Iran, since they consider all ophiolites along this belt as supra-subduction zone ophiolites, where the fore-arc, or arc and/or back-arc geochemical characteristics dominate, while Khoy ophiolites is taken as a mid-ocean spreading ridge remnant (after Khalatbari Jafari *et al*., 2003).

Mobasher *et al.* (2002) reported the displacement of the Khoyophiolites due to thrusting over metamorphic rocks. This was based on DEM generation (digital elevation model) from Terra satellite.

More recently Avagyan *et al.* (2016) advanced the idea of allochthonousnature for the non-metamorphic ophiolites of the Khoy area. They correlate the stratigraphy and structural features of the Khoy area with those form the Armenian ophiolites along the Sevan-Akera suture. They report similarities between stratigraphy and tectonics of the South Armenian Block (SAB) and Khoy area.

The most important similarities are as follows. Pre-Late Cretaceous stratigraphy in both the areas are similar. The Permian and Triassic stratigraphic successions in the Khoy region are similar to that of the Gondwana-related basement in the SAB (Avagyan *et al.,* 2016).

Metamorphism in the Khoy area (Azizi *et al*., 2011) and the SAB (Baghdasarian and Ghukasian, 1983; Hässig *et al.,* 2013) are comparable. The absence of Lower Middle Devonian and Upper Carboniferous deposits can be seen in both SAB and the Khoy area.

The supra-subduction geochemical features of the Khoy non-metamorphic ophiolites are consistent with the previously proposed geodynamic setting for the ophiolites along the Sevan-Akera suture in the Lesser Caucasus (Galoyan *et al.,* 2007 ;Rolland *et al.,* 2009; Sosson *et al.,* 2010; Hässig *et al.,* 2013). OIB-type alkaline rocks in the Armenian ophiolites suggests the emplacement of an oceanic plateau during the late Aptian (Rolland *et al.,* 2009).OIB-type rocks are reported from the Khoy area (Moazzen and Oberhansli, 2008).

Considering all these observations, Avagyan *et al.* (2016) concluded that Khoy allochthonous non-metamorphic ophiolites continue to the north and were obducted along the Sevan-Akera suture zone. This suture zone is a continuation of Izmir-Ankara–Erzincan suture (e.g. Hässig *et al.,* 2013).

The studied ophiolitic rocks from the Dizajaland area are similar to ophiolites along the Izmir-Ankara-Erzincan suture in Turkey (Sarifakio lu *et al*., 2010; Parlak *et al.,* 2013), ophiolites along Sevan-Akera suture zone in Armenia (Rolland *et al.,* 2009; Sosson *et al.*, 2010; Hässig *et al.,* 2013) and "Inner Ophiolite Belt" of Iran (Shafaii Moghadam and Stern, 2014). Formation of ophiolites in a supra-subduction zone is commonly attributed to further melting of depleted mantle by injection of hydrous melts above subduction zones (*Kubo et al*., 2002, Ghazi *et al*., 2012).These types of ophiolites are far better represented and preserved than MORB ophiolites in the orogenic belts. Late Cretaceous ophiolites, located along the Neotethys suturein the Middle East, show both supra-subduction zone and abyssal geochemical features. This testifies to their formations in arc tectonic settings (Ricou, 1971; Parkinson *et al*., 1992; Glennie, 2000). Robertson (2002) considered the major Cretaceous ophiolites of the Mediterranean and Middle East as intra-oceanic subduction zones. Two parallel ophiolitic belts in Iran known as 'Inner' and 'Outer' ophiolitic belts are continued towards the NW in Turkey, where they appear as 'North Ophiolite Belt' and 'South Ophiolite Belt'. Due to complex nature of geology of the Khoy area and different geotectonic settings proposed for the ophiolites (e.g. oceanic ridge, Khalatbari Jafari *et al*., 2003; back-are basin, Monsef *et al.,* 2010; fore-arc basin, Moazzen *et al*., 2012 and this study), relating the Khoy ophiolites to either northern or southern branches of the southern Neotethys has been debated. Our findings on tectonic setting of the non-metamorphic Khoy ophiolites based on whole rock chemistry and mineral chemistry of mafic and ultramafic rocks from the Dizajaland area along with correlations made by Avagyan *et al.* (2016) and information provided on east Turkey ophiolites (Göncüoglu, 2014; Colako lu *et al.,* 2014, Sarifakio lu *et al*., 2010; Parlak *et al.,* 2013) shows that most likely the Khoy ophiolite marks the continuation of the Izmir-Ankara-Erzican suture, probably displaced to the present location allochthonously from the Sevan-Akera suture as the northerly continuation of the Izmir-Ankara-Erzincan suture.

Conclusions

The present study on petrography and chemistry of mafic and ultramafic rock from the Dizajaland area on non-metamorphic Khoy ophiolite and comparing with other studies lead us to the following conclusions.

(1) The main rock types of the Dizajaland area are serpentinized peridotites, serpentine, gabbro, diabase, spilitic pillow lava, radiolarian chert and Santonian-Campanian pelagic limestone. These represent a dismembered sequence of the non-metamorphic Khoy ophiolitic complex in NW Iran.

(2) Whole rock chemistry of basalt, diabase and gabbro samples are characterized by calc-alkaline (gabbro), and tholeiitic (basalt and diabase) nature for the rocks. Basalt and gabbro samples show mainly E-MORB features, while diabasic samples have N-MORB nature. These mafic rocks show dual geochemical features indicative of mafic rocks formed at mid-ocean ridge and those formed in a subduction zone. These mixed features are taken as a supra-subduction zone setting for the ophiolite.

(3) Chemistry of orthopyroxene in the peridotites shows a supra-subduction and fore-arc setting for the Dizajaland rocks. Spinel composition confirms a fore-arc setting for these rocks and defines a mantle array for the peridotites.

(4) Tectonic setting of the non-metamorphic Khoy ophiolites, based on this study and comparing it with tectonic setting of ophiolites from Armenia, east Turkey and "Inner Ophiolitic Belt" of Iran shows that most likely the Khoy ophiolite marks the continuation of the Izmir-Ankara-Erzincan suture, apparently at its north branch of Sevan-Akera suture, from which the Khoy ophiolite is displaced allochthonously.

Acknowledgments

We sincerely thank Ms. Mahleqa Rezaei Bargoshadi for her help with microprobe analyses. Mrs. Nassrin Rahbar Saadat from ZPS Company Iran, helped with whole rock analyses arrangement. We would like to thank the editor of the journal and the respectful reviewers for their helps and comments.

References

Alavi M. (1991): Sedimentary and structural characteristics of the Paleo-Tethys remnants in northeastern Iran. Geological Society of American Bulletin 103: 983-992.

Amini B. Radfar J. Khalatbari M. and Behrudi A. (1993): Geological map of the Dizajaland Quadrangle, Scale1/100000, Geological Survey of Iran.

Arai S. (1987): An estimation of the least depleted spinel peridotite on the basis of olivine–spinel mantle array. Neues Jahrbuchfür Mineralogie Monatshefte 8:347–354.

Arai S. (1994a): Characterization of spinel peridotites by olivine–spinel compositional relationships. review and interpretation. Chemical Geology 113:191– 204.

Arai S. (1994b): Compositional variation of olivine–chromian spinel in Mg-rich magmas as a guide to their residual spinel peridotites. Volcanology and Geothermal Research 59, :279–293.

Arvin M. and Robinson P.T. (1994): Petrogenesis and tectonic setting of lavas from the Baftophiolitic mélange, southwest of Kerman, Iran. Canadian journal of Earth Sciences 31:824 -834.

Avagyan A. Shahidi A. Sosson M. Sahakyan, L. Galoyan G. Muller, C. Vardanyan S. Firouzi K.B. Bosch D. Danelian T. and Asatryan G. (2016): New data on the tectonic evolution of the Khoy region, NW Iran. Geological Society, London, Special Publications, 428, 428-13.

Azizi H. Chung S-L. Tanaka T. and Asahara Y. (2011): Isotopic dating of the Khoy metamorphic complex (KMC), northwestern Iran. A significant revision of the formation age and magma source. Precambrian Research 185:87–94.

Baghdasarian G.P. and Ghukasian R. Kh. (1983): The age of Bdjnimigmatite-granitic massif by the Rb-Sr isochrones radiometric data and geological ideas. Izvestia NAS of Armenian SSR, Nauki o Zemle, 6: 15–29 [in Russian].

Bogaard P. J. F. and Worner G. (2003):Petrogenesis of basanitic to tholeiitic volcanic rocks from the Miocene Vogelsberg central Germany.Journal of Petrology 44:569-602.

Bogoch R. Avigad D. and Weissbrod T. (2002): Geochemistry of the Quartz diorite granite association, Roded area, southern Israel. Journal of African Earth Sciences 35:51-59.

Choi S.H. Shervais J.W. and Mukasa S.B. (2008): Supra-subduction and abyssal mantle peridotites of the Coast Range ophiolite, California.

Contributions to Mineralogy and Petrology 156:551–576.

Çolakoglu A.R. Günay K. Göncüoglu M.C. Oyan V. and Erdogan K. (2014): Geochemical evaluation of the Late Maastrichtian subduction-related volcanism in the southern Neotethys in Van area, and a correlation across the Turkish-Iranian border. Ofioliti 39:51-65.

Conrad W.K. and Kay R.W. (1984): Ultramafic and mafic inclusions from Adak Island. crystallization history and implications for the nature of primary magmas and crustalevolution in theAleutian arc. Journal of Petrology 25:88-125.

Dilek Y. Furnes H. and Shallo M. (2007): Supra subduction zone ophiolite formation along the periphery of Mesozoic Gondwana. Gondwana Research 11:453–475.

Fitton J. G. Hardarson B.S. Ellam R.M. and Rogers G. (1998): Sr, Nd, and Pb- isotopic composition of volcanic rocks from the southeast Greenland Margin at 63-N.Temporal variation in crustal contamination during continental breakup. In. Saunders A.D., Larsen H. C., Wise S.H., (Eds.), Proc. ODP, Scientific Results, 152. College Station, (Ocean Drilling Program), 351-357.

Floyd P.A. Yaliniz M.K. and Goncuoglu M.C. (1998): Geochemistry and petrogenesis of intrusive and extrusive ophiolitic plagiogranites, Central Anatolian Crystalline Complex, Turkey. Lithos 42:225-241.

Galoyan G. Rolland Y. Sosson M. Corsini M. and Melkonyan R. (2007): Evidence for superposed MORB, oceanic plateau and volcanic arc series in the Lesser Caucasus (Stepanavan, Armenia). C.R. Geoscience 339: 482–492.

Ghazi A.M. and Hassanipak A. A. (2000): Petrology and geochemistry of the Shahr-Babakophiolite, Central Iran. Geological Survey of America, Special paper 349:485-497.

Ghazi J. M. Moazzen M. Rahgoshay M. and Shafaii Moghadam H. (2010): Mineral chemical composition and geodynamic significance of peridotites from Nain ophiolite, central Iran. Journal of Geodynamics 49, 261–270.

Ghazi J. M. Moazzen M. Rahgoshay M. and Shafaii Moghadam H. (2011): The geodynamic setting of the Nainophiolites, Central Iran. Evidence from chromianspinels in the chromitites and associated rocks. Ofioliti 36:59-76.

Ghazi J. M. Moazzen M. Rahgoshay M. and Shafaii Moghadam H. (2012): Geochemical characteristics of basaltic rocks from the Nain ophiolite (Central Iran); constraints on mantle wedge source evolution in an oceanic back arc basin and a geodynamical model. Technophysics 29:92–104.

Glennie K. W. (2000): Cretaceous tectonic evolution of Arabia's eastern plate margin. a tale of two oceans. In. Middle East Models of Jurassic/Cretaceous Carbonate Systems (eds. A. S. Alsharan and R. W. Scott), 9–20. Society of Economic Paleontologists and Mineralogists (SEPM) Special Publication no. 69.

Göncüoglu M. C. (2014): Comments on a single versus multi-armed Southern Neotethys in SE Turkey and Iran. The Third International Symposium of the International Geoscience Programme Project 589. 19-26 Oct. 2014, Tehran- Iran

Haggerty S.E. (1988): Upper mantle opaque mineral stratigraphy and the genesis of metasomatites and alkali-rich melts. Journal of Geological Society of Australia 14:687–699.

Hajialioghli R. and Moazzen M. (2014): Supra-subduction and mid-ocean ridge peridotites from the Piranshahr area, NW Iran. Journal of Geodynamics 81:41–55.

Hassanipak A. and Ghazi M. (2000): Petrology, geochemistry and tectonic setting of the Khoy ophiolite, North West Iran. implications for Tethyan tectonics. Journal of Asian Earth Sciences 18: 109-121.

Hässig, M. Rolland Y. Sosson M. Galoyan G. Muller C. Avagyan A. and Sahakyan L. (2013): New structural and petrological data on the Amasia ophiolites (NW Sevan-Akera suture zone, Lesser Caucasus). Insights for a large-scale obduction in Armenia and NE Turkey. Tectonophysics 588:135–153.

Ishii T. Robinson P.T. Maekawa H. and Fiske R. (1992): Petrological studies of peridotites from diapiric serpentinite seamounts in the Izu–Ogasawara–Mariana Forearc, Leg 125. In. Fryer O., Pearce J.A., Stokking L.B. (Eds.), Proceedings of the Ocean Drilling Program, Scientific Results, 125. Ocean Drilling Program, College Station: 445–485.

Johnson K. T. M. Dick H. J. B. and Shimizu N. (1990): Melting in the oceanic upper mantle; an ion microprobe study of diopsides in abyssal peridotites. Journal of Geophysical Research 95:2661-2678.

Kamenov B. (2004): The olivine basalts from Livingston Island, west Antractica. Petrology and geochemical comparisions. Bulgarian Academy of Sciences, Geochemistry, Mineralogy and Petrology 41:71-98.

Kepezhinskas P. K. Defant M. J. and Drummond M. S. (1995): Na metasomatism in the island-arc mantle by slab melt-peridotite interaction. evidence from mantle xenoliths in the North Kamchatka arc. Journal of Petrology 36:1505-1527.

Khalatbari Jafari M. Juteau T. Bellon H. and Emami H. 2003: Discovery of two ophiolite complexes of different ages in the khoyarea (NW Iran), Comptes Rundes Geoscience 335: 917-929.

Khalatbari Jafari M. Juteau T. Bellon H. Whitechurch H. Cooton J. and Emami H. (2004): New geological, geochronological and geochemical investigation on the Khoyophiolites and related formations, NW Iran, Journal of Asian Earth Sciences 23: 507-535.

Knipper A. Ricou L.E. and Dercourt J. (1986): Ophiolites as indicators of the geodynamic evolution of the Tethyan ocean. Technophysics123 :213-240.

Kubo T. Ohtani E. Kondo T. Kato T. Toma M. Hosoya T. Sano A. Kikegawa T. and Nagase T. (2002): Metastable garnet in oceanic crust at the top of the lower mantle. Nature 420: 803-806.

Moazzen M. Alchalan S. Hajialioghli R. Morishita T. and Rezaei M. (2012): Ophiolitic peridotites from the Western Khoy ophiolitic complex, NW Iran; Petrological and geochemical characteristics and application for connecting the Baft-Khoy and Izmir-Ankara-Erzincan sutures. Inter. Earth Sci. Colloq. Aegean Region, 1-5 October, 2012, Dokuz Eylul University, Izmir, Turkey.

Moazzen M. and Oberhänsli R. (2008): Whole rock and relict igneous clinopyroxene geochemistry of ophiolite-related amphibolites from NW Iran-Implications for protolith nature. Neues Jahrbuchfür Mineralogie Abhandlungen 185:51-62.

Mobasher K. Hendrix E. Babaei H. and Yin Z. (2002): Structural GIS Analyses of the Khoy Ophiolite Complex, Northwestern Iran. Denver Annual Meeting, 183.

Monsef I. Rahgoshay_M. Mohajjel M. and Shafaii Moghadam H. (2010): Peridotites from the Khoy Ophiolitic Complex, NW Iran. Evidence of mantle dynamics in a supra-subduction-zone context. Journal of Asian Earth Sciences 38:105–120.

Omrani H. Moazzen M. Oberhänsli R. Tsujimori T. Bousquet R. and Moayyed M. (2013): Metamorphic history of glaucophane-paragonite-zoisiteeclogites from the Shanderman area, northern Iran. Journal of Metamorphic Geology 31:791–812.

Parkinson I.J. Pearce J.A. Thirlwall M.F. Johnson K.T.M. and Ingram G. (1992): Trace element geochemistry of peridotites from the Izu–Bonin–Mariana forearc Leg125. In. Fryer, P., Pearce, J.A., Stokking, L.B., et al., (Eds.), Proceedings of the Ocean Drilling Program – Scientific Results. 125, College Station, TX, 487–506.

Parlak O. Çolako lu A. Dönmez C. Sayak H. Yildirim N. Türkel and A. Odaba i . (2013): Geochemistry and tectonic significance of ophiolites along the zmir–Ankara–Erzincan Suture Zone in northeastern Anatolia. Geological Society, London, Special Publications, 372(1):75-105.

Pearce J.A. and Cann, J.R. (1973): Tectonic setting of basic volcanic rocks determined using trace element analyses. Earth and Planetary Science Letters 19:290–300.

Pearce J.A. (2008): Geochemical fingerprinting of oceanic basalts with applications to ophiolite classification and the search for Archean oceanic crust. Lithos 100:14–48.

Pearce J.A. (1982): Trace element characteristics of lavas from destructive plate boundaries. Andesites 8:525-548.

Radfar J. Amini B. and Khalatbari M. (1993): Geological Map of the Khoy Quadrangle, Scale 1/100,000. Geological Survey of Iran.

Ricou, L.E. 1971. Le croissant ophiolitiqueperi-arabe.uneceinture de nappesmisesen place au Cretacé supérieur. Rev. Géogr. Phys. Géol. Dyn. 13:327–349.

Robertson A. (2002): Overview of the genesis and emplacement of Mesozoic ophiolites in the Eastern Mediterranean Tethyan region. Lithos 65:1-67.

Rolland R. Galoyan G. Bosch D. Sosson M. Corsini M. Fornari M. and Verati C. (2009): Jurassic back-arc and Cretaceous hot-spot series in the Armenian ophiolites – implications for the obduction process. Lithos 112:63–187.

Rollinson H.R. (2009):New models for the genesis of plagiogranites in the Oman ophiolite. Lithos 112:603-614.

Sar fak o lu E. Özen H. Çolako lu A. and Sayak H. (2010): Petrology, mineral chemistry, and tectonomagmatic evolution of Late Cretaceous suprasubduction zone ophiolites in the zmir–Ankara–Erzincan suture zone, Turkey. International Geology Review 52: 187-222.

Saunders A.D. Storey M. Kent R. and Norry M.

(1992): Consequences of plume-lithosphere interactions. Geological Society of London Special Publications 68:41-60.

Sengor A. M. C. and Natalin B. A. (1996): Paleotectonics of Asia. fragments of a synthesis. In. The Tectonic Evolution of Asia, 486-641 edited by. Yin A., Harrison M.

Shafaii Moghadam H. and Stern R. J. (2014): Ophiolites of Iran. Keys to understanding the tectonic evolution of SW Asia. (I) Paleozoic ophiolites. Journal of Asian Earth Sciences 91:19–38.

Sosson M. Rolland Y. *et al.* (2010): Subductions-obduction and collision in the Lesser Caucasus (Armenia, Azerbaijan, Georgia), new insights. In.Sosson, M., Kaymakci, N., Stephenson, R., Bergerat, F. & Starostenko, V. (eds) Sedimentary Basin Tectonics from the Black Sea and Caucasus to the Arabian Platform. Geological Society, London, Special Publications 340, 329–352.SP340.14

Sun S.S. (1980): Lead isotopic study of young volcanic rocks from mid-ocean ridges, ocean islands and island arcs. Philosophical Transactions of the Royal Society of London A. Mathematical, Physical and Engineering Sciences 297:409-445.

Sun S.S. and McDonough W.F. (1989): Chemical and isotopic systematics of oceanic basalts. In. Saunders A.D., Norry M.J. (Eds.). Magmatism in the Ocean Basins. Geological Society of London Special Publication 42:313–345.

Thirwall F. M. Upton B. G. J. and Jenkins C. (1994): Interaction between continental lithosphere and Iceland plume. Sr-Nd- Pb isotope geochemistry of Tertiary basalts, NE Greenland. Journal of Petrology 35:839- 879.

Topuz G. Gocmengil G. Rolland Y. Celik O.F. Zack T. and Schmitt, A. K. (2013): Jurassic accretionary complex and ophiolite from northeast Turkey. No evidence for the Cimmerian continental ribbon. Geology 41:255-258.

Wilson M. (1989): Igneous petrogenesis- A global tectonic approach. Unwin Hyman Lond. England.

Zanetti A. Mazzucchelli M. Rivelenti, G. &Vannunci R. (1999): The Finerophlogopite-peridotite Massif: an example of subduction-related metasomatism. Contribution to Mineralogy and Petrology. 134:107-122.